Terrigenous Mass Movements

Detection, Modelling, Early Warning and Mitigation Using Geoinformation Technology

Bearbeitet von
Biswajeet Pradhan, Manfred Buchroithner

1. Auflage 2012. Buch. viii, 400 S. Hardcover
ISBN 978 3 642 25494 9
Format (B x L): 15,5 x 23,5 cm
Gewicht: 771 g

Chapter 2
Landslide Susceptibility Mapping Using a Spatial Multi Criteria Evaluation Model at Haraz Watershed, Iran

H. R. Pourghasemi, Biswajeet Pradhan, Candan Gokceoglu and K. Deylami Moezzi

Abstract The purpose of this study is to prepare landslide susceptibility map using a spatial multi criteria evaluation approach (SMCE) in a landslide-prone area (Haraz) in Iran. In the first stage, landslide locations were identified in the study area from interpretation of aerial photographs, and field surveys. In the second stage, twelve data layers were used as landslide conditioning factors for susceptibility mapping. These factors are slope, aspect, altitude, lithology, land use, distance from rivers, distance from roads, distance from faults, topographic wetness index, stream power index, stream transport index, and plan curvature. Next, landslide-susceptible areas were analyzed using the SMCE approach and mapped using landslide conditioning factors. For verification, the results of the analyses was compared with the field-verified landslide locations. Additionally, the receiver operating characteristics (ROC) curves for all landslide susceptibility models were drawn and the area under curve values was calculated. Landslide locations were used to validate results of the landslide susceptibility map generated using the SMCE approach and the verification results showed a 76.84% accuracy. According to the results of the AUC evaluation, the produced map has exhibited good performance.

Keywords Landslide · Susceptibility · GIS · Remote sensing · Spatial multi criteria evaluation · AHP · Iran

H. R. Pourghasemi · K. Deylami Moezzi
Department of Watershed Management Engineering,
College of Natural Resources and Marine Sciences, Tarbiat Modares University,
International Campus, Noor, Iran

B. Pradhan (✉)
Institute of Advanced Technology, Spatial and Numerical Modeling Laboratory, University Putra Malaysia, 43400 Serdang, Selangor, Malaysia
e-mail: biswajeet24@gmail.com; biswajeet@lycos.com

C. Gokceoglu
Applied Geology Division, Department of Geological
Engineering, Engineering Faculty, Hacettepe University, Ankara, Turkey

B. Pradhan and M. Buchroithner (eds.), *Terrigenous Mass Movements*,
DOI: 10.1007/978-3-642-25495-6_2,

2.1 Introduction

Undesired effects on human life and economic activity resulting from landslides are observed throughout the world. During the 1990's, nearly nine percent of worldwide natural disasters constitutes of landslides (Gokceoglu et al. 2005). According to Schuster and Fleming (1986), in many countries, the economic losses and causalities due to landslides are greater than commonly recognized and generate a yearly loss of property larger than that from any other natural disaster, including earthquakes, floods and windstorms.

Over the last decade, it is possible to find many studies on landslide susceptibility assessment. The basic concept was first introduced by Radbruch (1970), Dobrovolny (1971), and Brabb and Pampeyan (1972) as the spatial distribution of factors related to the instability processes in order to determine zones of landslide-prone areas without any temporal implication. Guzzetti et al. (1999) summarized most of the landslide susceptibility mapping studies. More recently, probabilistic models have been proposed (Dai and Lee 2001; Gokceoglu et al. 2005; Akgun and Bulut 2007; Akgun et al. 2008; Lee and Pradhan 2007; Oh and Lee 2009). The logistic regression model has also been employed for landslide susceptibility mapping (Nefeslioglu et al. 2008; Pradhan 2010a; Chauhan et al. 2010; Bai et al. 2010; Akgun 2011). Shou and Wang (2003) and Zhou et al. (2003) have used the geotechnical and factor of safety parameter models to investigate the slope failure of the studied areas. Data mining using fuzzy logic, artificial neural network and decision tree models have also been applied in Geographical Information Systems (GIS) as a new landslide susceptibility assessment approach (e.g. Ercanoglu and Gokceoglu 2002, 2004; Ermini et al. 2005; Lee et al. 2006; Melchiorre et al. 2006; Castellanos and VanWesten 2007; Kanungo et al. 2006; Wang 2008; Tangestani 2009; Wan 2009; Saito et al. 2009; Pradhan 2010a, b, c, 2011; Pradhan et al. 2010; Pradhan and Buchroithner 2010, Pradhan and Lee 2009, 2010a, b, c; Akgun and Turk 2010; Nefeslioglu et al. 2010; Yeon et al. 2010; Sezer et al. 2011; Akgun 2011), multicriteria decision analysis (MCDA) approach (Ayalew et al. 2005; Komac 2006; Akgun and Balut 2007; Yalcin 2008; Akgun and Turk 2010; Akgun 2011). In this study, a GIS based spatial multi criteria model was used for landslide susceptibility mapping at Haraz watershed.

2.2 Study Area

The study area is located in the northern part of Iran, which is one of the most landslide prone areas in Iran (Pourghasemi 2008). The watershed area centered between the longitudes of 52° 06′ 02′ E to 52° 18′ 13″ E, and latitudes of 35° 49′ 05″ N to 35° 57′ 39″ N, is mountainous and is located in the Alborz Folded geological zone (Fig. 2.1). It covers two adjacent 1:50,000 topographic sheets of

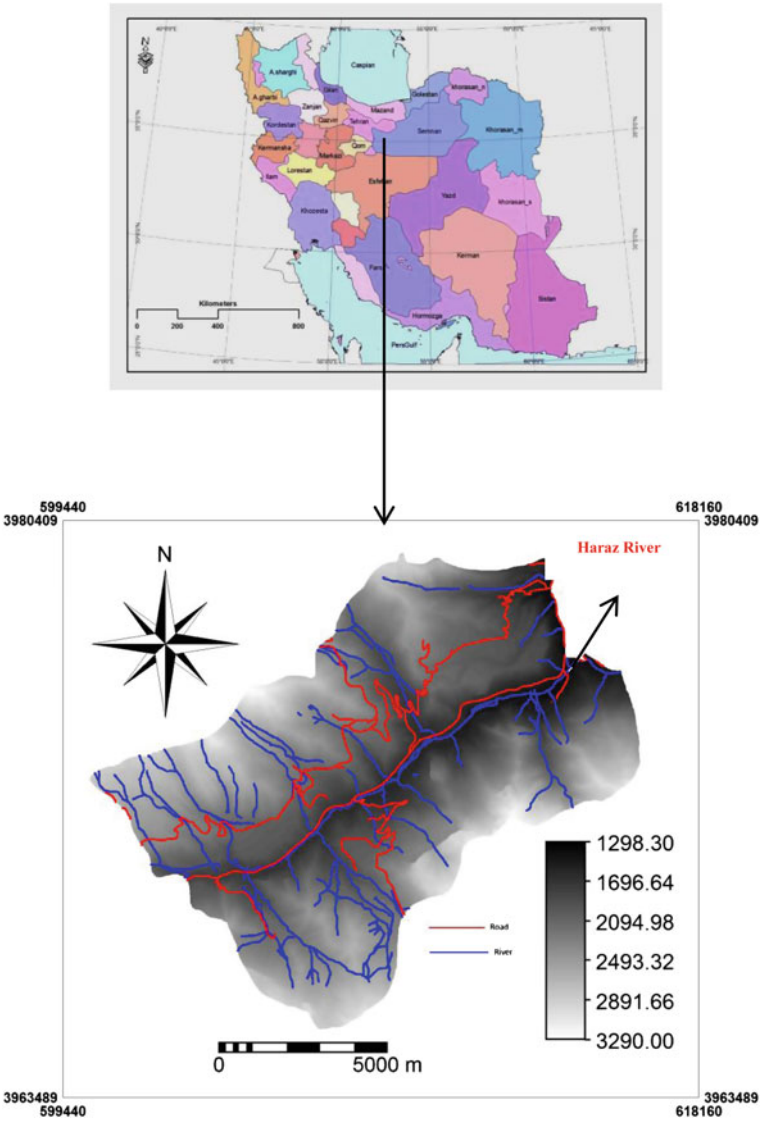

Fig. 2.1 Location of the study area showing Mazandaran province in Iran

the Army Geographic Institute of Iran and has an extent of about 114.5 km^2. In the study area, the main river is the Haraz. Based on the data from the Iranian Meteorological Department, the temperature in the study area varies between −25°C in winter and 36.5°C in summer. The mean annual rainfall is around 500 mm, while the maximum precipitation falls between November and January in general. Altitude values in the study area vary between 1200 to 3290 m.asl.

2.3 Methodology

In general, decision analysis uses a set of systematic procedures for analyzing complex decision problems. The basic strategy is to divide the decision problem into small, understandable parts, analyze each of them, and integrate these parts in a logical manner to produce a meaningful solution (Malczewski 1999). To solve spatial-based problems such as geo-hazards (landslide, erosion, earthquakes) and site selection, GIS-based spatial multi criteria evaluation (SMCE) have been used.

SMCE is a way of producing policy-relevant information about spatial decision problems for decision makers. An SMCE problem can be visualized as an evaluation table of maps or as a map of evaluation tables, as shown in Fig. 2.2 (Sharifi and Herwijnen 2003). According to Sharifi and Retsios (2004) if the objective of the evaluation is a ranking of the alternatives, then the evaluation table of maps has to be transformed into one final ranking of alternatives. Actually, the function has to aggregate not only the effects but also the spatial component (Sharifi and Herwijnen 2003). At times, defining such a function can be highly complicated. Therefore, it is required to simplify the function by dividing it into at least two operations. Those operations are: (i) aggregation of the spatial component, and (ii) aggregation of the criteria. These two operations can be carried out in different orders as visualized in Fig. 2.3 as Path 1 and Path 2. These two path features resembles the order of aggregation. If we consider a step wise analysis during the first path, then the first step is the aggregation across spatial units (spatial analysis is the principal tool); the second step is the aggregation across criteria (multi criteria analysis playing the main role). Similarly, in the second path, these steps are taken in reverse order. In the first case, the effect of one alternative for one criterion is a map (Sharifi and Retsios 2004; Sharifi and Herwijnen 2003). This case can be used when evaluating the spatial evaluation problem using the so-called 'Path 1'. In the second case, every location has its own zero-dimensional problem and can best be used when evaluating the spatial problem using the so-called 'Path 2' (Fig. 2.3). For implementing the whole semi-quantitative model the SMCE module of ILWIS-GIS (integrated land and water information system) was used (Castellanos, 2008). The SMCE application assists and guides users in doing multi-criteria evaluation in a spatial manner (ITC 2001). The model is built by making criteria tree, where the conditioning parameter maps are grouped, standardized and weighted. The landslide casual parameters are weighted by means of direct, pair-wise, and rank ordering comparison and the output is a composite index map (Castellanos and Van Westen 2007). Figure 2.4 presents an overview of the various components of the landslide susceptibility method.

In this study a pair-wise comparison based weighting was used. This method assumes that the users comparably evaluate the difference of magnitude among all unique pairs of factors qualitatively. Pair-wise comparison method was established by Saaty (1980) in the context of the analytical hierarchy process (AHP). In this process, the weights are defined by standardizing the eigenvector correlated with the highest eigenvalue of the ratio matrix. The AHP consists of three main steps;

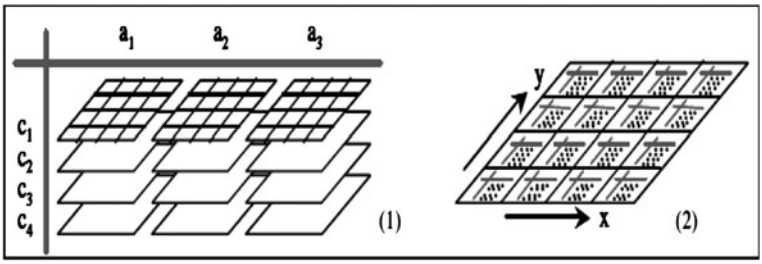

Fig. 2.2 Two interpretations of a two-dimensional decision problem (*1*: table of maps, *2*: map of tables); *Source* Sharifi and Retsios 2004)

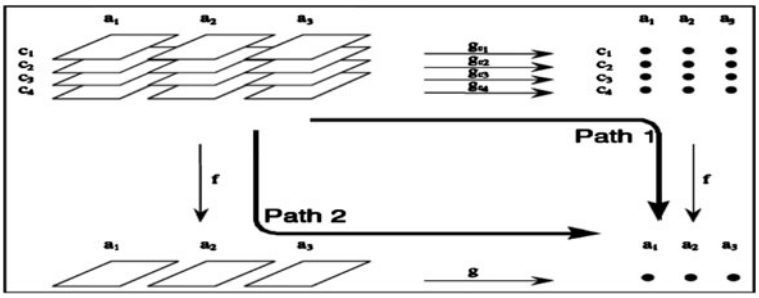

Fig. 2.3 Two paths of spatial multi criteria evaluation (adapted from Herwijnen 1999). The result of both path 1 and 2 is a ranking of alternatives a1, a2, and a3, with respect to their performance in terms of the four spatial effects (criteria c1, c2, c3, and c4) for which they are evaluated (functions f) and the spatial distribution of these effects, which is aggregated in functions g. (*Source* Sharifi and Retsios 2004)

1) generating the pair wise comparison matrix, 2) computing the weights of the criterion, and 3) estimating the consistency ratio (Malczewski 1999). In the development of comparison matrix, the method employs an underlying scale with values from 0 to 1 to rate the relative preferences for two criteria which can be seen in the Table 2.1.

This study used the combination between bivariate statistical analysis and pair-wise comparison. Firstly, to know the scored value for each class parameter, we calculated the density of landslides by using some steps in the bivariate statistical analysis (frequency ratio model). The second process is grouping the conditioning factors into four induced factors such as geomorphological, geological, hydrological and anthropogenic.

Next, the levels of weight values were used to standardize the input value by means of pair wise comparison resulting values from 0 to 1. After this process the steps in spatial multi criteria evaluation were followed again by means of pair-wise comparison method. The difference of this improved method was located on

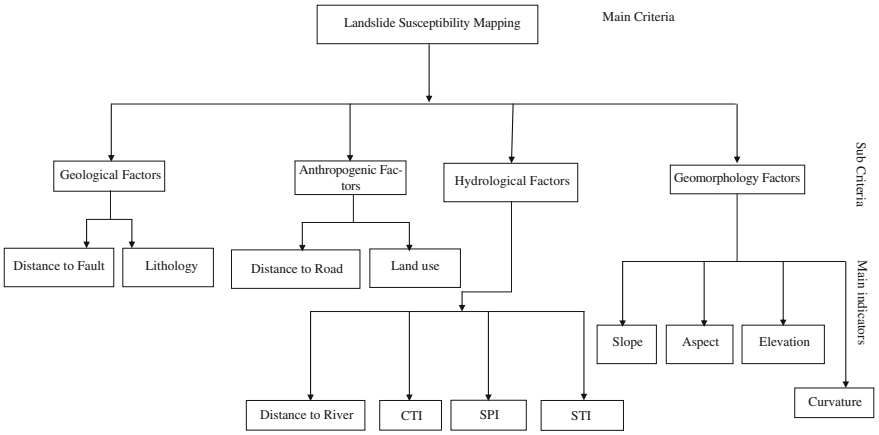

Fig. 2.4 The methodological flow chart showing the step wise processes for landslide susceptibility mapping in Haraz watershed

Table 2.1 Scale of relative importance suggested by Saaty (1997)

Inensity of importance	Definition	Explanation
1	Equal importance	Two activities contribute equally to objective
3	Weak importance of one over another	Experience and judgment slightly favor one activity over another
5	Essential or strong importance	Experience and judgment strongly favor one activity over another
7	Demonstrated importance	An activity is strongly favored and its dominance demonstrated in practice
9	Absolute importance	The evidence favoring one activity over another is the highest possible order of affirmation
2, 4, 6, 8	Intermediate values between the two adjacent judgments	When compromise is needed

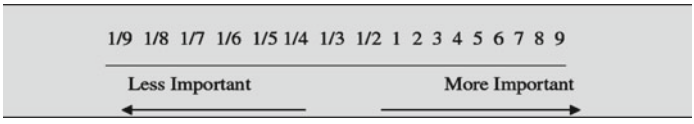

giving the weighting value of each parameter. The weighting value of this method was given by calculation process of analytical hierarchy process (AHP). The values were extracted based on the level of influences. Expert opinion which depends on observed physical characteristic of landslide sites determined the levels of the influencing factors.

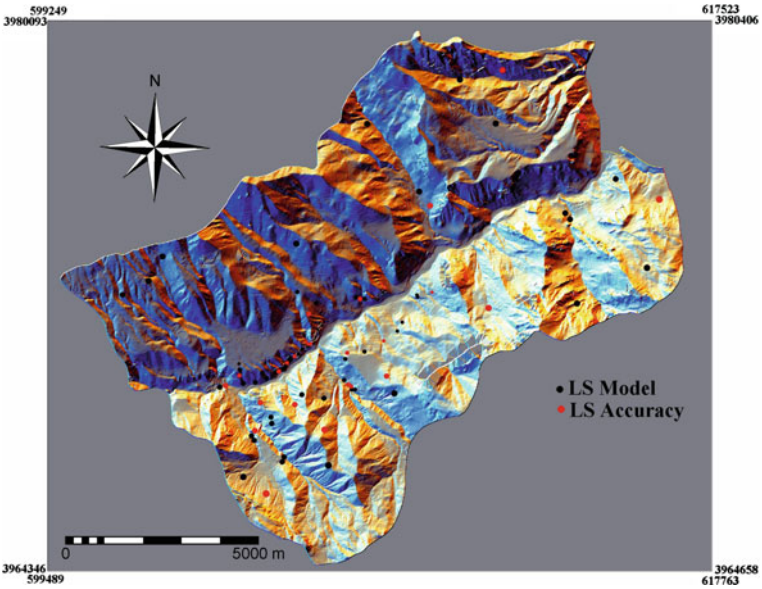

Fig. 2.5 Landslide distribution map of the study area

2.4 Construction of Spatial Database

2.4.1 Landslide Inventory Map

The existing landslide inventory map is very essential for studying the relationship between the landslide distribution and the conditioning factors. To produce a detailed and reliable landslide inventory map, extensive field surveys and observations were performed in the study area. A total of 78 landslides were identified and mapped in the study area by evaluating aerial photos at 1:25,000 scale and by multiple field studies (Fig. 2.5). The modes of failure for the landslides identified in the study area were determined according to the landslide classification system proposed by Varnes (1978).

2.4.2 Slope

The most important parameter in the slope stability analysis is the slope angle (Lee and Min 2001). Because the slope angle is directly related to the landslides and it is frequently used in preparing landslide susceptibility maps (Clerici et al. 2002; Saha et al. 2005; Cevik and Topal 2003; Ercanoglu and Gokceoglu 2004; Lee et al. 2004a; Lee 2005; Yalcin 2005). For this reason, the slope map of the

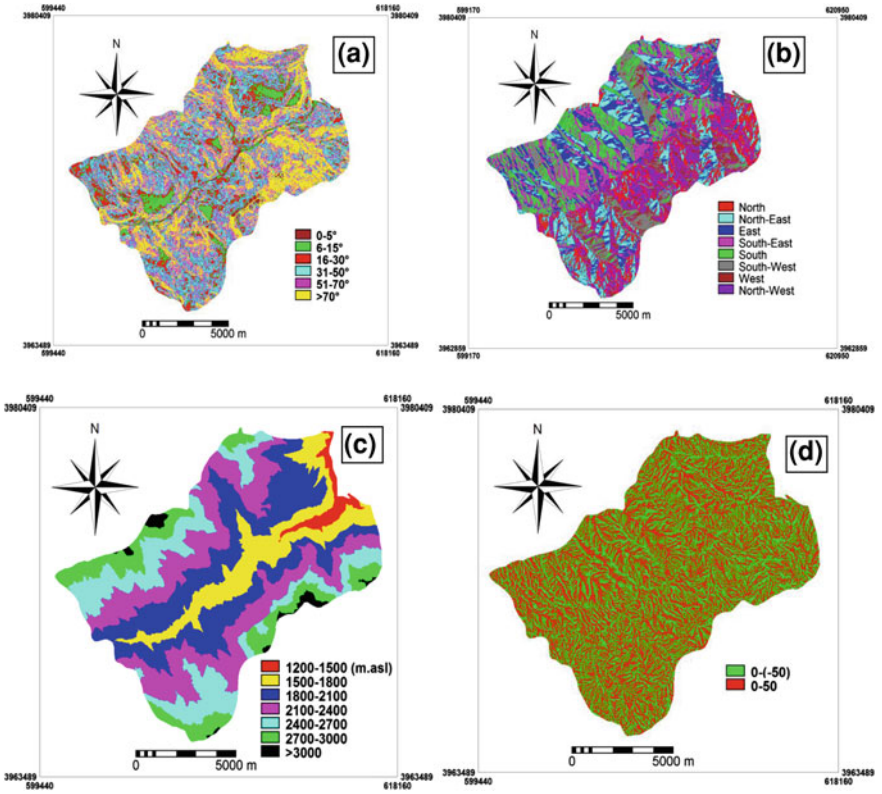

Fig. 2.6 Topographical parameter maps of the study area; **a** slope (degree), **b** aspect, **c** altitude (m.asl), **d** plan curvature

study area is prepared from the DEM, and divided into six slope categories (Fig. 2.6a). The spatial relationship between slope and landslide are presented in Table 2.2.

2.4.3 Aspect

Aspect is also considered as a landslide conditioning factor, and this parameter has been considered in several other studies (Van Westen and Bonilla 1990; Gokceoglu and Aksoy 1996; Saha et al. 2005; Ercanoglu and Gokceoglu 2004; Lee et al. 2004a, b; Yalcin 2005). Some of the meteorological events such as the direction of the rainfall, amount of sunshine, the morphologic structure of the area affect the slope stability (Mohammadi 2008). The hillsides receiving dense rainfall reach saturation faster, however this is also related to infiltration capacity of the slope controlled by various parameters such as topographic slope, type of soil,

Table 2.2 Spatial relationship between landslides and landslide conditioning factors

Factor	Class	No. of pixels in domain	Percentage of domain	No. of landslide	Percentage of landslide	Frequency ratio	a	b	c	d
Slope (Deg)	0–5	13851	1.21	1	1.82	1.50	0.9	0.325	0.181	0.053
	6–15	64268	5.62	2	3.64	0.65	0.1	0.325	0.181	0.006
	16–30	155602	13.59	10	18.18	1.34	0.75	0.325	0.181	0.044
	31–50	343634	30.03	19	34.55	1.15	0.57	0.325	0.181	0.034
	51–70	262117	22.91	10	18.18	0.79	0.23	0.325	0.181	0.014
	>70	304809	26.64	13	23.64	0.89	0.33	0.325	0.181	0.019
Aspect	North	149997	13.12	5	9.09	0.69	0.28	0.067	0.181	0.003
	Northeast	195301	17.07	9	16.36	0.96	0.41	0.067	0.181	0.005
	East	129167	11.29	2	3.64	0.32	0.1	0.067	0.181	0.001
	Southeast	171144	14.95	16	29.09	1.95	0.9	0.067	0.181	0.011
	South	135677	11.85	3	5.46	0.46	0.17	0.067	0.181	0.002
	Southwest	131718	11.51	9	16.36	1.42	0.64	0.067	0.181	0.008
	West	79979	6.99	7	12.73	1.82	0.84	0.067	0.181	0.01
	Northwest	151298	13.22	4	7.27	0.55	0.21	0.067	0.181	0.003
Altitude (m)	1200–1500	28463	2.49	0	0	0	0.1	0.107	0.181	0.002
	1500–1800	157018	13.72	19	34.54	2.52	0.9	0.107	0.181	0.017
	1800–2100	303058	26.48	22	40	1.51	0.58	0.107	0.181	0.011
	2100–2400	305844	26.73	7	12.73	0.48	0.25	0.107	0.181	0.005
	2400–2700	208321	18.20	6	10.91	0.60	0.29	0.107	0.181	0.006
	2700–3000	125384	10.96	1	1.82	0.17	0.15	0.107	0.181	0.003
	>3000	16193	1.42	0	0	0	0.1	0.107	0.181	0.002
Lithology	A	459914	40.19	30	54.55	1.36	0.9	0.833	0.267	0.2
	B	153621	13.43	3	5.45	0.41	0.34	0.833	0.267	0.076
	C	147386	12.88	2	3.64	0.28	0.26	0.833	0.267	0.058
	D	19655	1.72	0	0	0	0.1	0.833	0.267	0.022
	E	363705	31.78	20	36.36	1.14	0.77	0.833	0.267	0.171

(continued)

Table 2.2 (continued)

Factor	Class	No. of pixels in domain	Percentage of domain	No. of landslide	Percentage of landslide	Frequency ratio	a	b	c	d
Land use	Best Range	246601	21.55	12	21.82	1.01	0.16	0.667	0.490	0.052
	Mixing orchard and agriculture	152518	13.33	20	36.36	2.73	0.41	0.667	0.490	0.134
	Residential	3450	0.30	1	1.82	6.07	0.9	0.667	0.490	0.294
	Moderate range	741712	64.82	22	40	0.62	0.1	0.667	0.490	0.033
Distance to faults	0–100 m	44942	3.93	3	5.45	1.39	0.31	0.167	0.267	0.014
	101–200 m	43132	3.77	4	7.27	1.93	0.52	0.167	0.267	0.023
	201–300 m	43144	3.77	6	10.91	2.89	0.9	0.167	0.267	0.04
	301–400 m	44914	3.92	2	3.64	0.93	0.13	0.167	0.267	0.006
	>400 m	968149	84.61	40	72.73	0.86	0.1	0.167	0.267	0.004
Distance to rivers	0–100 m	263584	23.03	33	60	2.61	0.9	0.132	0.062	0.007
	101–200 m	205759	17.98	5	9.09	0.51	0.15	0.132	0.062	0.0012
	201–300 m	159801	13.97	7	12.73	0.91	0.29	0.132	0.062	0.002
	301–400 m	131420	11.49	3	5.45	0.47	0.13	0.132	0.062	0.001
	>400 m	383717	33.53	7	12.73	0.38	0.1	0.132	0.062	0.0008
Distance to roads	0–100 m	136228	11.90	23	41.82	3.51	0.9	0.333	0.490	0.147
	101–200 m	110283	9.64	4	7.27	0.75	0.16	0.333	0.490	0.026
	201–300 m	93440	8.17	5	9.10	1.11	0.25	0.333	0.490	0.041
	301–400 m	83876	7.33	3	5.45	0.74	0.15	0.333	0.490	0.024
	400–500 m	74626	6.52	3	5.45	0.84	0.18	0.333	0.490	0.029
	>500 m	645828	56.44	17	30.91	0.55	0.1	0.333	0.490	0.016
TWI	0–4	144529	12.63	50	90.91	7.20	0.9	0.377	0.062	0.021
	4–8	983621	85.96	4	7.27	0.08	0.11	0.377	0.062	0.003
	8–12	16077	1.40	1	1.82	1.3	0.24	0.377	0.062	0.006
	>12	54	0.005	0	0	0	0.1	0.377	0.062	0.002

(continued)

Table 2.2 (continued)

Factor	Class	No. of pixels in domain	Percentage of domain	No. of landslide	Percentage of landslide	Frequency ratio	a	b	c	d
SPI	0–20	266962	23.33	15	27.27	1.17	0.9	0.422	0.062	0.024
	20–40	267926	23.42	12	21.82	0.93	0.26	0.422	0.062	0.007
	40–60	191325	16.72	8	14.55	0.87	0.1	0.422	0.062	0.003
	60–80	130680	11.42	6	10.91	0.96	0.34	0.422	0.062	0.009
	80–100	87780	7.67	4	7.27	0.95	0.31	0.422	0.062	0.008
	>100	199608	17.44	10	18.18	1.04	0.55	0.422	0.062	0.014
STI	0–10	271966	23.77	16	29.09	1.22	0.73	0.070	0.062	0.003
	10–20	362255	31.66	17	30.91	0.98	0.53	0.070	0.062	0.002
	20–30	267619	23.39	12	21.82	0.93	0.49	0.070	0.062	0.002
	30–40	139582	12.20	5	9.09	0.75	0.34	0.070	0.062	0.001
	40–50	58732	5.13	4	7.27	1.42	0.9	0.070	0.062	0.004
	>50	44127	3.85	1	1.82	0.47	0.1	0.070	0.062	0.0004
Plan curvature	Concave	553227	48.35	21	38.18	0.79	0.1	0.501	0.181	0.009
	Convex	591054	51.65	34	61.82	1.20	0.9	0.501	0.181	0.082

Domain: pixels in study area, domain (%): (domain/total pixels in study area)* 100, landslide: number of landslide occurrences, landslide (%): (landslide/total number of landslide occurrences) *100 and frequency ratio: landslide (%)/domain (%).

$A = Q^{sc}, Q_2^t$ and Q_1^t, $B = Q^{ag}, Q^{ta}, Q^{tu}$ and Q^b, $C = K_k^{tv}$ and E_k^{gy}, $D = PE_z$ and PE_f, $E = K_2, K_t, J_1, J_d, J_S, TR_{el}$ and P_d.

a: Normalized Value, b: parameter's Value, c: Group's Value, d: Final Weight

permeability, porosity, humidity, the organic ingredients, land cover, and the climatic season. As a result, pore water pressure of the slope-forming material increases. Consequently, in this study, the aspect map of the study area is produced to show the relationship between aspect and landslide (Fig. 2.6b).

2.4.4 Altitude

Altitude is also a significant landslide conditioning factor because it is controlled by several geologic and geomorphological processes (Gritzner et al. 2001; Dai and Lee 2002; Ayalew et al. 2005; Pourghasemi 2008). To assess altitude as an input parameter for the landslide susceptibility map, an altitude map is prepared from the 10m × 10mdigital elevation model (Fig. 2.6c).

2.4.5 Plan Curvature

The term curvature is theoretically defined as the rate of change of slope gradient or aspect, usually in a particular direction (Wilson and Gallant 2000). The curvature value can be evaluated by calculating the reciprocal value of the radius of curvature of that particular direction. Hence, while the curvature values of broad curves are small, the tight ones have higher values. Plan curvature is described as the curvature of a contour line formed by intersecting a horizontal plane with the surface. The influence of plan curvature on the slope erosion processes is the convergence or divergence of water during downhill flow. For this reason, this parameter constitutes one of the conditioning factors controlling landslide occurrence (Nefeslioglu et al. 2008). The plan curvature map was produced using the script written by Hengl et al. (2003) and run in ILWIS 3.3 software (Fig. 2.6d).

2.4.6 Lithology

Landslides are greatly controlled by the lithology properties of the land surface. Since different lithologic units have different landslide susceptibility values, they are very important in providing data for susceptibility mapping. For this reason, it is essential to group the lithologic properties properly (Carrara et al. 1991; Anbalagan 1992; Mejia-Navarro and Wohl 1994; Mejia-Navarro and Garcia 1996; Pachauri et al. 1998; Luzi and Pergalani 1999; Dai et al. 2001; Yalcin 2005; Duman et al. 2006).

Therefore, a lithology map of the study area is digitized from the existing geology map (sheet number 6461) at the scale of 1:100,000 from the Geological

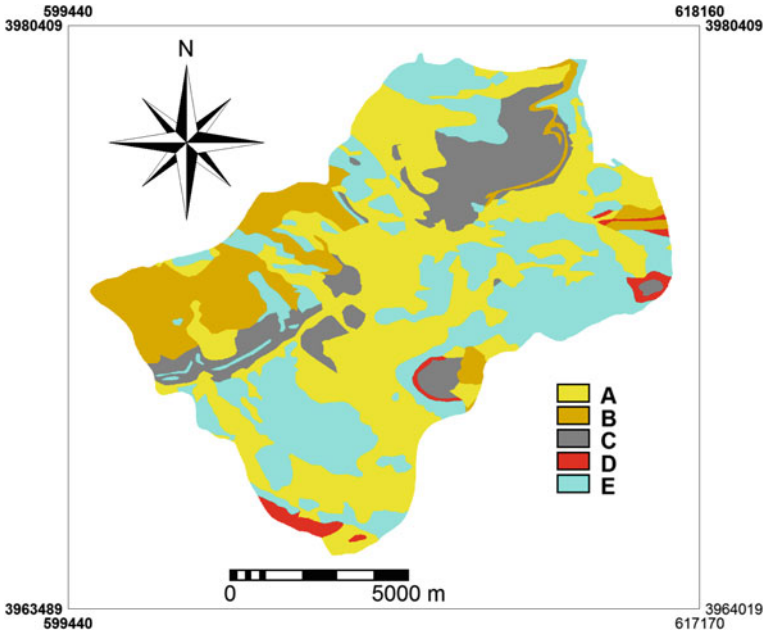

Fig. 2.7 The lithology map of the study area

Survey of Iran (GSI). The study area is covered with various types of lithologic formations. The general geological setting of the area is shown in Fig. 2.7, and the lithological properties are summarized in Tables 2.2 and 2.3.

2.4.7 Land Use

In this study, a land use map was prepared from the LANDSAT satellite image by applying a supervised classification scheme and field surveys. There are four types of landuse are identified in the study area: best range, moderate range, mixed orchard and agriculture and residential areas (Fig. 2.8). Most of the study area is covered by moderate range (64.32%). Several researchers (Maharaj 1993; Fernandez et al. 1999; Jakob 2000; Ocakoglu et al. 2002) emphasized on the importance of vegetation cover or land use characteristics on the stability of slopes, and they considered vegetation cover to assess the conditioning factors of landslides. For the study area, the spatial relationship between land use factor and landslide occurrence are presented in Table 2.2.

Table 2.3 Geology formation of research area

Code	Class	Formation	Lithology	Geological age
Q^{sc}	A	–	Scree	Quaternary
$Q_2{}^t$		–	Young terraces	Quaternary
$Q_1{}^t$		–	Old terraces	Quaternary
Q^{ag}	B	–	Agglomerate	Quaternary
Q^{ta}		–	Trachy andesitic lava flows	Quaternary
Q^{tu}		–	Ash tuff, lapilli tuff	Quaternary
Q^b		–	Olivine basalt	Quaternary
$K_k{}^{tv}$	C	Karaj	Green tuff, basaltic and limestone with gypsum and conglomerate	Eocene
$E_k{}^{gy}$		Karaj	Gypsum	Eocene
PE_z	D	Ziarat	Limestone bearing nummulites and alveolina, conglomerate	Paleocene
PE_f		Fajan	Conglomerate, agglomerate, some marl and limestone	Paleocene
K_2	E	–	Biogenic and cherty limestone	Late Cretaceous
K_t		Tizkuh	Orbitoline bearing limestone	Late Cretaceous
J_1		Lar	Massive to well bedded, cherty limestone	Late Jurassic
J_d		Dalichai	Well bedded, partly oolitic-detritic limestone, marly limestone	Late Jurassic
J_S		Shemshak	Dark shale and sandstone with plant remains, coal	Late Jurassic
TR_{eL}		Elika	Thin bedded limestone	Early Triassic
P_d		Dorud	Cross bedded, quartzitic sandstone	Early Permian

2.4.8 Distance from Rivers

An important parameter that controls the stability of a slope is the saturation degree of the material on the slope. The closeness of the slope to drainage structures is another important factor in terms of stability. Streams may adversely affect stability by eroding the slopes or by saturating the lower part of material until resulting in water level increases (Gokceoglu and Aksoy 1996). Five different buffer zones are created within the study area to determine the degree to which the streams affected the slopes (Fig. 2.9).

2.4.9 Distance from Roads

Similar to the effect of the distance to streams, landslides may occur on the road and on the side of the slopes affected by roads (Pachauri and Pant 1992; Pachauri et al. 1998; Ayalew and Yamagishi 2005; Yalcin 2005). A road constructed beside slopes causes a decrease in the load on both the topography and on the toe of slope.

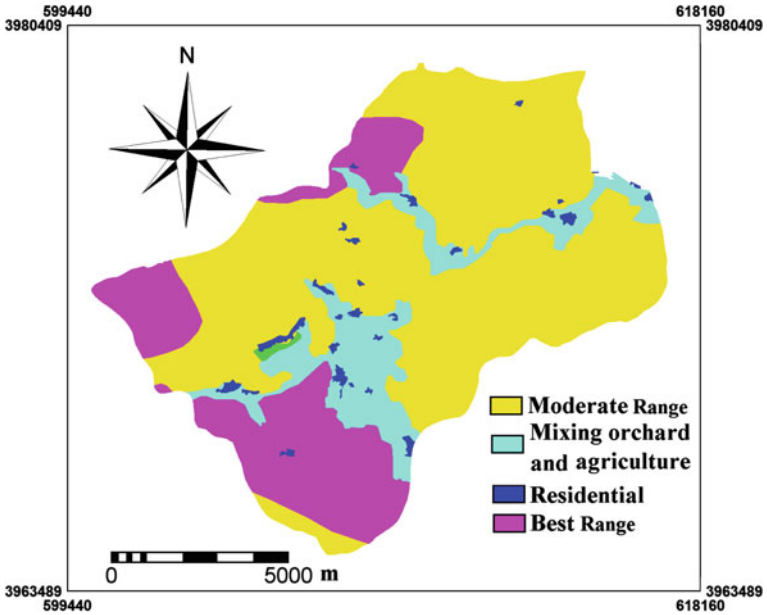

Fig. 2.8 The land use map of the study area

As a result of an increase in stress on the back of the slope, because of changes in topography and decrease of load on toe, some tension cracks may develop. Although a slope is balanced before the road construction, some instability may be observed because of negative effects of excavation. In fact, during the field works, some landslides were recorded whose origin can be attributed to road construction. For this reason, five different buffer areas are created on the path of the road to determine the effect of the road on the stability of slope (Fig. 2.10). The landslide percentage distribution and its frequency ratio are determined considering the distance classes to the road achieved by comparing the map of the distance to the road and the landslide inventory (Table 2.2).

2.4.10 Distance from Faults

The distance from fault is calculated at 100 m intervals using the lithology map (Fig. 2.11). Faults form a line or zone of weakness characterized by heavily fractured rocks. Selective erosion and movement of water along fault planes promote such phenomena. Besides the major thrusts and faults on the geological maps complementary information regarding possible faults and structural dislocations were recognized as lineaments by means of image enhancement (filtering) of satellite imagery. The recognition of lineaments as possible faults is performed

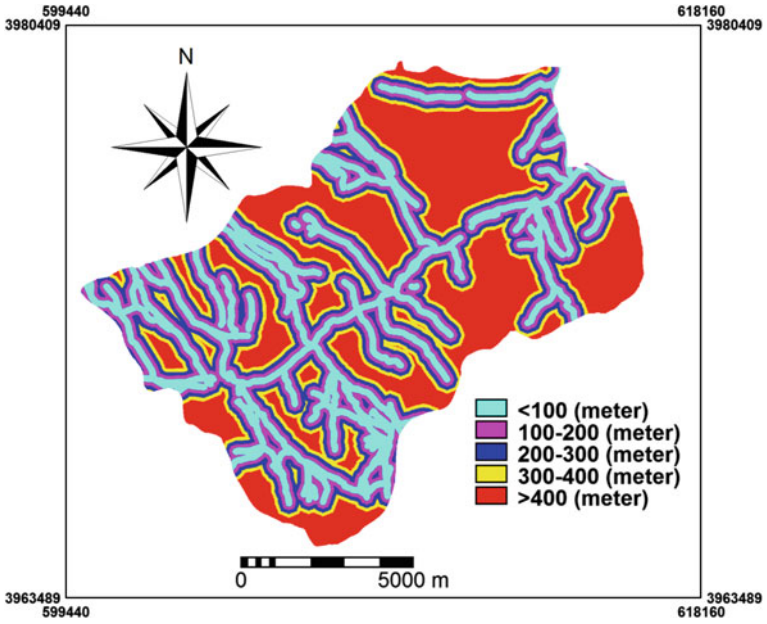

Fig. 2.9 The distance from rivers map of the study area

step-by-step form large to smaller scales allowing the generalization of many neighboring small order lineaments taking into account the spatial scale of the study. The spatial relationship between distance from faults and landslide are presented in Table 2.2.

2.4.11 Topographic Wetness Index (TWI)

The topographic wetness index (TWI) has been used extensively to describe the effect of topography on the location and size of saturated source areas of runoff generation. Moore et al. (1991) proposed Eq. (2.1) for the calculation of TWI under the assumption of steady state conditions and uniform soil properties (i.e. transmisivity is constant throughout the catchment and equal to unity).

$$TWI = \ln(A_S / \tan \beta) \tag{2.1}$$

where A_S is the specific catchment's area (m^2/m), and β is slope gradient (in degrees).

According to Wood et al. (1990), the variation in the topographical components is often far greater than the local variability in soil transmisivity, and Eq. (2.1) can be used to calculate TWI. The TWI map was produced using the script written by Hengl et al. (2003) and run in ILWIS 3.3 software (Fig. 2.12a).

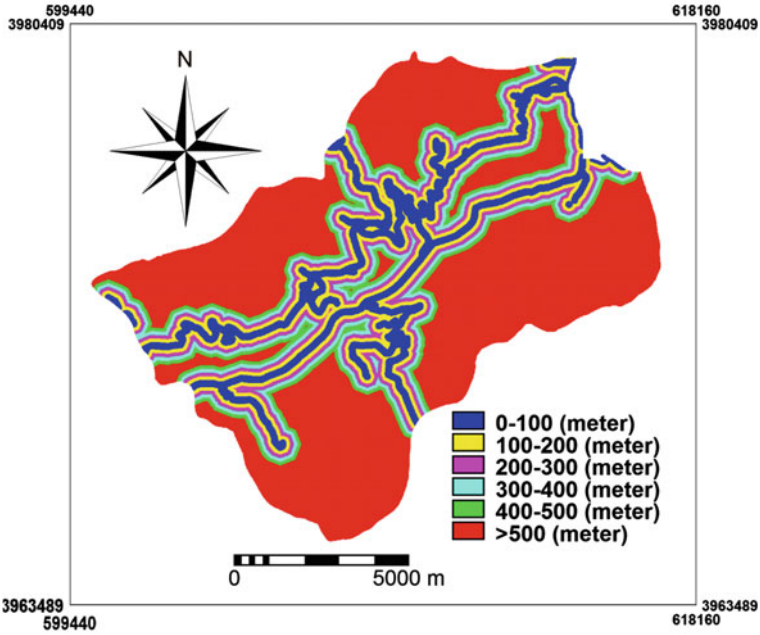

Fig. 2.10 The distance from roads map of the study area

2.4.12 Stream Power Index (SPI)

The stream power index (SPI) is a measure of the erosive power of water flow based on the assumption that discharge (q) is proportional to specific catchment area (As) (Eq. 2.2) (Moore et al. 1991).

$$SPI = A_S \times \tan \beta \tag{2.2}$$

where A_S is the specific catchment's area (m^2/m), and β the slope gradient in degrees. As the specific catchment's area and gradient increase, the amount of water contributed by upslope areas and the velocity of water flow increase; hence, the SPI and slope-erosion risk increase (Moore et al. 1991). Moore et al. (1993) stated that the SPI controls the potential erosive power of overland flow. Therefore, these processes can be considered as one of the components of landslide occurrence (Lee and Min 2001; Gokceoglu et al. 2005; Nefeslioglu et al. 2008; Yilmaz 2009; Akgun and Turk 2010). The SPI map was produced using the script written by Hengl et al. (2003) and run in ILWIS 3.3 software (Fig. 2.12b).

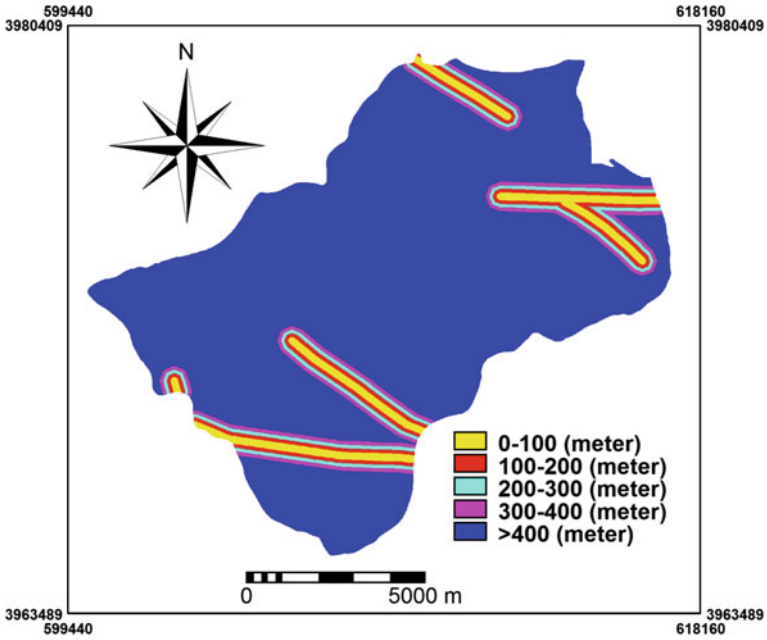

Fig. 2.11 The distance from faults map of the study area

2.4.13 Stream Transport Index (STI)

Another index often used to reflects the erosive power of the overland flow is the sediment transport index (Moore et al. 1993). The STI is calculated from the following formula:

$$STI = \left(\frac{A_S}{22.13}\right)^{0.6} \left(\frac{\sin \beta}{0.0896}\right)^{1.3} \tag{2.3}$$

where A_S is the specific catchment's area (m^2/m), and β the slope gradient.

This empirical formula resembles the Universal Soil Loss Equation and can thus be used to depict locations of potential erosion risk (Moore and Burch 1986). If a close inspection on Eq. (2.3) is performed, it is revealed that the physical meaning of this factor is the capability of sediment transportation controlled a specific catchment area and slope gradient. For that reason, the main causes for this phenomenon may be the disturbed drainage system and the low slope gradient trend on landslide bodies. Therefore, this distinct anomaly can be considered as a good indicator of landslide occurrence (Nefeslioglu et al. 2008). The STI map was produced using the script written by Hengl et al. (2003) and run in ILWIS 3.3 software (Fig. 2.12c).

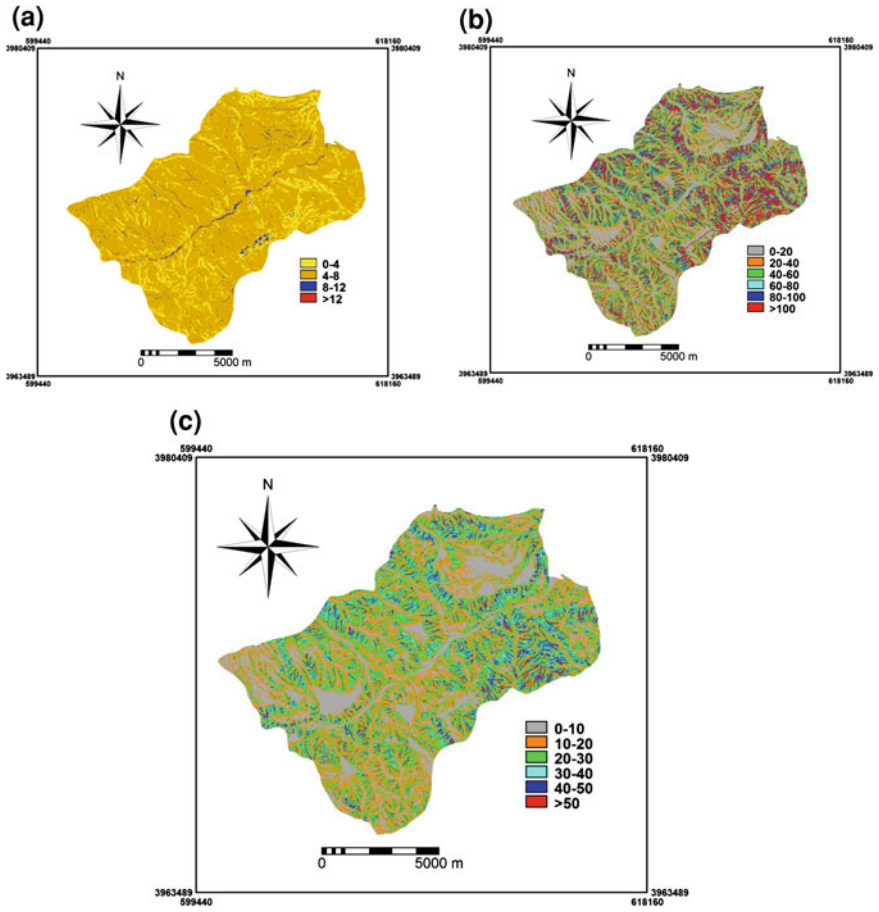

Fig. 2.12 Hydrological based terrain maps of the study area; **a** TWI, **b** SPI, **c** STI

The spatial relationship between TWI, SPI, STI, and landslide occurrence are presented in Table 2.2.

2.5 Landslide Susceptibility Mapping

In this study, the employed SMCE method was built based on analyzing the weight value in bivariate statistical analysis (Table 2.2). All comparisons are based on pair-wise method published by Saaty (1980) in terms of analytical hierarchy process. In this method, all factors were classified into a few groups. The first group consists of slope, aspect, altitude and plan curvature parameters; the second one includes lithology and distance from faults parameters which were extracted

from geological map. The next groups presenting the hydrological condition contains of distance from rivers, topographical wetness index (TWI), stream power index (SPI) and stream transport index (STI) parameters and the last group consists of land use and distance from roads parameters, because both of these were induced by human activities. The level of influence for groups and parameters were determined by the range of weighting and were determined by the range of weighting values between a spectrum from minimum to maximum. The range value is between the minimum and maximum weight value. The standardization of each class parameter is compared to each other in order to determine the level of influence. Normalized priority value for each class parameter had been extracted by following Eq. (2.4):

$$N_V = 0.8\left(\frac{X_i - X_{Min}}{X_{Max} - X_{Min}}\right) + 0.1 \tag{2.4}$$

The final weight values were automatically calculated by means of spatial multi criteria evaluation in ILWIS software. The final weight value for each class parameter is produced by multiplying the group weight value, parameter weight value and normalized priority value of class parameter (Table 2.2). Based on weighting values in AHP, the levels of the influence of parameters were generated. The anthropogenic factor has the most influence and the hydrological factor which has the less influence and was categorized in the lowest level. Pair-wise comparison method (Table 2.1) was performed to extract the weight value as presented in Table 2.4.

Based on total weight value, the susceptibility map for Haraz watershed was constructed (Fig. 2.13).

2.6 Validation of the Landslide Susceptibility Map

Validation is a fundamental step in the development of a susceptibility and determination of its prediction ability. The prediction capability of a landslide susceptibility model is usually estimated by using independent information that is not available for building the model. An alternative way to the above statistics is the threshold (cut-off value) calculations, is the receiver operating characteristic (ROC) value and the area under the ROC curve (AUC) (Zweig and Campbell 1993). This method has been widely used as a measure of performance of a predictive rule (Yesilnacar and Topal 2005; Van Den Eeckhaut et al. 2006; Baeza et al. 2010). ROC plots the different accuracy values obtained against the whole range of possible threshold values of the functions, and the AUC serves as a global accuracy statistic for the model, regardless of a specific discriminate threshold. This curve is obtained by plotting all combinations of sensitivities and proportions of false negatives (1-specificity) which may be obtained by varying the decision threshold. The range of values of the ROC curve area is 0.5–1 for a good-fit, while

Table 2.4 The weight value for each group and parameter using pair-wise comparison for SMCE

Number	Groups and parameters	The weight value	Inconsistency ratio
1	Geomorphologic factor	0.181	
	Slope	0.325	
	Aspect	0.067	0.09
	Altitude	0.107	
	Plan curvature	0.501	
2	Geological factor	0.267	
	Lithology	0.833	0.00
	Distance to fault	0.167	
3	Hydrological factor	0.062	
	Distance to river	0.132	
	Topographic wetness index	0.377	0.09
	Stream power index	0.422	
	Stream Transport Index	0.070	
4	Human induced	0.490	
	Land use	0.667	0.00
	Distance to road	0.333	

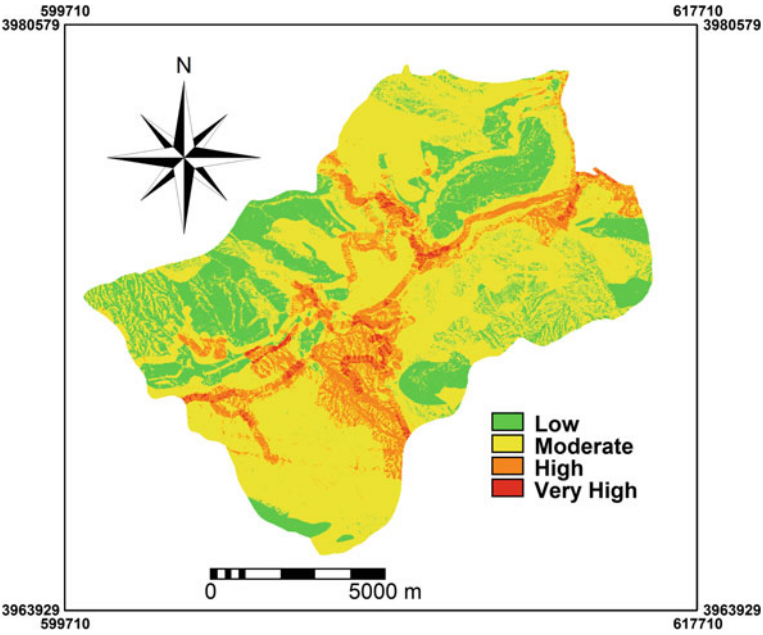

Fig. 2.13 Landslide susceptibility map produced by spatial multi criteria evaluation

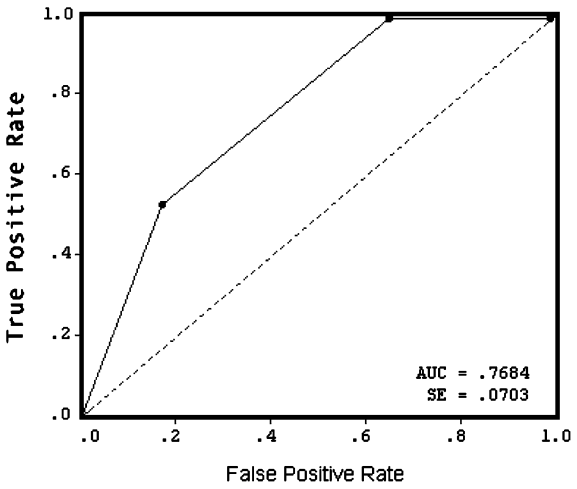

Fig. 2.14 ROC curve for the SMCE

values below 0.5 represent a random fit (Hanley and McNeil 1983). Figure 2.14 shows the ROC curve of the spatial multi criteria evaluation model for the training sample. The AUC value is 0.7684, indicate the good ability of function to correctly discriminate between failed and unfailed groups in the sample used for building the model.

2.7 Concluding Remarks

The landslide susceptibility map prepared in the present study is the result of a combination of various factors responsible for landslide susceptibility, in which each factor has relative importance to probable landslide activity. A reliable and accurate susceptibility map depends on the inclusion and proper determination of the role of these parameters. In this study, twelve landslide-controlling parameters, namely slope, aspect, altitude, plan curvature, land use, lithology, distance from rivers, distance from roads, distance from faults, topographic wetness index, stream power index and stream transport index, were considered. Subsequently, landslide-susceptible areas were analyzed by the SMCE approach and mapped using landslide conditioning factors. For the purpose of verification, the learning set of landslides was randomly sampling choose from a total of 78 landslides population disregarding the temporal component. The ROC curve of block entry SMCE was produced based on the test data set, which was randomly collected from landslide bodies and safe zones. The results showed a 76.84% accuracy with standard error of 0.0703. According to the results of the AUC evaluation, the produced map has exhibited promising results.

References

Akgun A (2011) A comparision of landslide susceptibility maps produced by logistic regression, multi-criteria decision, and likelihood ratio methods: a case study at Izmir, Turkey. Landslides doi:10.1007/s10346-011-0283-7

Akgun A, Bulut F (2007) GIS-based landslide susceptibility for Arsin-Yomra (Trabzon, 381 North Turkey) region. Environ Geol 51:1377–1387

Akgun A, Dag S, Bulut F (2008) Landslide susceptibility mapping for a landslide-prone area (Findikli, NE of Turkey) by likelihood frequency ratio and weighted linear combination models. Environ Geol 54(6):1127–1143

Akgun A, Turk N (2010) Landslide susceptibility mapping for Ayvalik (Western Turkey) 379 and its vicinity by multicriteria decision analysis. Env Earth Sci 61(3):595–611

Anbalgan R (1992) Land hazard evaluation and zonation mapping in mountainous terrain. Eng Geol 32:269–277

Ayalew L, Yamagishi H (2005) The application of GIS-based logistic regression for landslide susceptibility mapping in the Kakuda-Yahiko Mountains, Central Japan. Geomorphology 65(1/2):15–31

Ayalew L, Yamagishi H, Marui H, Kanno T (2005) Landslide in Sado Island of Japan: Part II. GIS-based susceptibility mapping with comparison of results from two methods and verifications. Eng Geol 81:432–445

Baeza C, Lantada N, Moya J (2010) Validation and evaluation of two multivariate statistical models for predictive shallow landslide susceptibility mapping of the Eastern Pyrenees (Spain). Environ Earth Sci 61:507–523

Bai S, Lü G, Wang J, Zhou P, Ding L (2010) GIS-based rare events logistic regression for landslide-susceptibility mapping of Lianyungang, China. Environ Earth Sci 62(1):139–149

Brabb EE, Pampeyan EH (1972) Preliminary map of landslide deposits in San Mateo County, California. US Geological Survey Miscellaneous Field Studies, Map MF-360, scale 1:62.500 (reprinted in 1978)

Carrara A, Cardinali M, Detti R, Guzzetti F, Pasqui V, Reichenbach P (1991) GIS techniques and statistical models in evaluating landslide hazard. Earth Surf Proc Land 16:427–445

Castellanos AEA (2008) Multi-Scale landslide risk assessment in Cuba. PhD thesis, ITC, ITC.Nl

Castellanos E, Van Westen CJ (2007) Generation of a landslide risk index map for Cuba using spatial multi-criteria evaluation. Landslide 4:311–325

Cevik E, Topal T (2003) GIS-based landslide susceptibility mapping for a problematic segment of the natural gas pipeline, Hendek (Turkey). Environ Geol 44:949–962

Chauhan S, Sharma M, Arora MK, Gupta NK (2010) Landslide susceptibility zonation through ratings derived from artificial neural network. Int J Appl Earth Observ Geoinf 12:340–350

Clerici A, Perego S, Tellini C, Vescovi P (2002) A procedure for landslide susceptibility zonation by the conditional analysis method. Geomorphology 48:349–364

Dai FC, Lee CF, Xu ZW (2001) Assessment of landslide susceptibility on the natural terrain of Lantau Island, Hong Kong. Environ Geol 40(3):381–391

Dai FC, Lee CF (2002) Landslide characteristics and slope instability modeling using GIS, Lantau Island, Hong Kong. Geomorphology 42:213–228

Dai FC, Lee CF (2001) Terrain-based mapping of landslide susceptibility using a geographical information systems: a case study. Can Geotech J 38:911–923

Dobrovolny E (1971) Landslide susceptibility in and near anchorage as interpreted from topographic and geologic maps, in the great Alaska earthquake of 1964-Geology volume. Publication 1603. U.S. Geological survey open file report 86-329, National Research Council, Committee on the Alaska Earthquake, National Academy of Sciences, USA, pp 735–745

Duman TY, Can T, Gokceoglu C, Nefeslioglu HA, Sonmez H (2006) Application of logistic regression for landslide susceptibility zoning of Cekmece Area, Istanbul, Turkey. Env Geol 51:241–256

Ercanoglu M, Gokceoglu C (2004) Use of fuzzy relations to produce landslide susceptibility map of a landslide prone area (West Black Sea Region, Turkey). Eng Geol 75:229–250

Ercanoglu M, Gokceoglu C (2002) Assessment of landslide susceptibility for a landslide-prone area (north of Yenice, NW Turkey) by fuzzy approach. Environ Geol 41:720–730

Ermini L, Catani F, Casagli N (2005) Artificial neural networks applied to landslide susceptibility assessment. Geomorphology 66:327–343

Fernández CI, Castillo TF, Hamdouni RE, Montero JC (1999) Verification of landslide susceptibility mapping: a case study. Earth Surf Proc Land 24(6):537–544

Gokceoglu C, Sonmez H, Nefeslioglu HA, Duman TY, Can T (2005) The 17 March 2005 Kuzulu landslide (Sivas, Turkey) and landslide-susceptibility map of its near vicinity. Eng Geol 81:65–83

Gokceoglu C, Aksoy H (1996) Landslide susceptibility mapping of the slopes in the residual soils of the Mengen region (Turkey) by deterministic stability analyses and image processing techniques. Eng Geol 44:147–161

Gritzner ML, Marcus WA, Aspinall R, Custer SG (2001) Assessing landslide potential using GIS, soil wetness modeling and topographic attributes, Payette River, Idaho. Geomorphology 37:149–165

Guzzetti F, Carrarra A, Cardinali M, Reichenbach P (1999) Landslide hazard evaluation: are view ofcurrent techniques and their application in a multi-scale study, Central Italy. Geomorphology 31:181–216

Hanley JA, McNeil BJ (1983) A method of comparing the areas under receiver operating characteristic curves derived from the same cases. Radiology 148:839–843

Hengl T, Gruber S, Shrestha DP (2003) Digital terrain analysis in ILWIS. International Institute for Geo-Information Science and Earth Oservation Enschede, The Netherlands, p 62

Herwijnen MV (1999) Spatial Decision Support for Environmental Management. Vrije Universiteit, Amsterdam 274

ITC (2001) ILWIS 3.0 academic-user's guide. ITC, Enschede, p 520

Jakob M (2000) The impacts of logging on landslide activity at Clayoquot Sound, British Columbia. Catena 38:279–300

Komac M (2006) A landslide susceptibility model using analytical hierarchy process method and multivariate statistics in perialpine-Slovenia. Geomorphology 74:17–28

Kanungo DP, Arora MK, Sarkar S, Gupta RP (2006) A comparative study of conventional, ANN black box, fuzzy and combined neural and fuzzy weighting procedures for landslide susceptibility zonation in Darjeeling Himalayas. Eng Geol 85(3–4):347–366

Lee S (2005) Application of logistic regression model and its validation for landslide susceptibility mapping using GIS and remote sensing data. Int J Remote Sens 26:1477–1491

Lee S, Choi J, Min K (2004a) Probabilistic landslide hazard mapping using GIS and remote sensing data at Boun, Korea. Int J Remote Sens 25:2037–2052

Lee S, Min K (2001) Statistical analysis of landslide susceptibility at Yongin, Korea. Environ Geol 40:1095–1113

Lee S, Pradhan B (2007) Landslide hazard mapping at Selangor, Malaysia using frequency ratio and logistic regression models. Landslides 4:33–41

Lee S, Pradhan B (2006) Probabilistic landslide risk mapping at Penang Island. Malays J Earth Syst Sci 115(6):1–12

Lee S, Ryu JH, Won JS, Park H (2004b) Determination and application of the weights for landslide susceptibility mapping using an artificial neural network. Eng Geol 71:289–302

Lee S, Ryu JH, Lee MJ, Won JS (2006) The application of artificial neural networks to landslide susceptibility mapping at Janghung, Korea. Math Geol 38(2):199–219

Luzi L, Pergalani F (1999) Slope instability in static and dynamic conditions for urban planning: the ''Oltre Po Pavese'' case history (Region Lombardia-Italy). Nat Hazards 20:57–82

Maharaj RJ (1993) Landslide processes and landslide susceptibility analysis from an upland watershed: a case study from St. Andrew, Jamaica, West Indies. Eng Geol 34: 53–79

Malczewski J (1999) GIS and multi criteria decision analysis. Wiley, New York. ISBN: 978-0-471-32944-2, p 408

Mejia-Navarro M, Garcia LA (1996) Natural hazard and risk assessment using decision support systems, application: Glenwood Springs, Colorado. Environ Eng Geosci 2(3):299–324
Mejia-Navarro M, Wohl EE (1994) Geological hazard and risk evaluation using GIS: methodology and model applied to Medellin, Colombia. Bull Assoc Eng Geol 31:459–481
Melchiorre C, Matteucci M, Remondo J (2006) Artificial neural networks and robustness analysis in landslide susceptibility zonation, IEEE. 2006 International Joint Conference on Neural Networks Sheraton Vancouver Wall Centre Hotel, Vancouver, 16–21 July, pp 4375–4381
Mohammadi M (2008) Mass movement hazard analysis and presentation of suitable regional model using GIS (Case Study: A part of Haraz Watershed), M.Sc. Thesis, Tarbiat Modarres University International Campus, Iran, p 80
Moore ID, Burch GJ (1986) Sediment transport capacity of sheet and rill flow: application of unit stream power theory. Water Res Res 22:1350–1360
Moore ID, Gessler PE, Nielsen GA, Peterson GA (1993) Soil attribute prediction using terrain analysis. Soil Sci Soc Am J 57:443–452
Moore ID, Grayson RB, Ladson AR (1991) Digital terrain modeling: a review of hydrological, geomorphological, and biological applications. Hydrol Process 5:3–30
Nefeslioglu HA, Sezer E, Gokceoglu C, Bozkir AS, Duman TY (2010) Assessment of landslide susceptibility by decision trees in the metropolitan area of Istanbul, Turkey, Mathematical Problems in Engineering, Article ID 901095, p 15, doi:10.1155/2010/901095
Nefeslioglu HA, Duman TY, Durmaz S (2008) Landslide susceptibility mapping for a part of tectonic Kelkit Valley (Eastern Black Sea region of Turkey). Geomorphology 94:401–418
Ocakoglu F, Gokceoglu C, Ercanoglu M (2002) Dynamics of a complex mass movement triggered by heavy rainfall: a case study from NW Turkey. Geomorphology 42(3):329–341
Oh HJ, Lee S, Chotikasathien W, Kim CH, Kwon JH (2009) Predictive landslide susceptibility mapping using spatial information in the Pechabun area of Thailand. Environ Geol 57: 641–651
Pachauri AK, Pant M (1992) Landslide hazard mapping based on geological attributes. EngGeol 32:81–100
Pachauri AK, Gupta PV, Chander R (1998) Landslide zoning in a part of the Garhwal Himalayas. Environ Geol 36(3–4):325–334
Pourghasemi HR (2008) Landslide hazard assessment using fuzzy logic (Case Study: A part of Haraz Watershed), M.Sc. Thesis, Tarbiat Modarres University International Campus, Iran, pp 92
Pradhan B (2010a) Remote sensing and GIS-based landslide hazard analysis and cross-validation using multivariate logistic regression model on three test areas in Malaysia. Adv Space Res 45(10):1244–1256
Pradhan B (2010b) Manifestation of an advanced fuzzy logic model coupled with Geoinformation techniques for landslide susceptibility analysis. Environ Ecol Stat 18(3):471–493
Pradhan B (2010c) Application of an advanced fuzzy logic model for landslide susceptibility analysis. Int J Comput Intell Sys 3(3):370–381
Pradhan B (2011) Use of GIS-based fuzzy logic relations and its cross application to produce landslide susceptibility maps in three test areas in Malaysia. Environ Earth Sci 63:329–349
Pradhan B, Buchroithner MF (2010) Comparison and validation of landslide susceptibility maps using an artificial neural network model for three test areas in Malaysia. Environ Eng Geosci 16(2):107–126
Pradhan B, Lee S (2009) Landslide risk analysis using artificial neural network model focusing on different training sites. Int J Phys Sci 3(11):1–15
Pradhan B, Lee S (2010a) Regional landslide susceptibility analysis using back-propagation neural network model at Cameron Highland, Malaysia. Landslides 7(1):13–30
Pradhan B, Lee S (2010b) Landslide susceptibility assessment and factor effect analysis: backpropagation artificial neural networks and their comparison with frequency ratio and bivariate logistic regression modeling. Environ Modell Softw 25:747–759
Pradhan B, Lee S (2010c) Delineation of landslide hazard areas using frequency ratio, logistic regression and artificial neural network model at Penang Island, Malaysia. Environ Earth Sci 60:1037–1054

Pradhan B, Sezer E, Gokceoglu C, Buchroithner MF (2010) Landslide susceptibility mapping by neuro-fuzzy approach in a landslide prone area (Cameron Highland, Malaysia). IEEE T Geosci Remote 48(12):4164–4177

Radbruch DH (1970) Map of relative amounts of landslides in California. US Geological Survey Open-File Report 70-1485, pp 36, map scale 1:500.000. US Geological Survey Open-File Report, pp 85–585

Saaty T (1980) The analytical hierarchy Process. McGraw-Hill, New York

Saaty TL (1997) A scaling method for priorities in hierarchical structures. J Math Psychol 15:234–281

Saha AK, Gupta RP, Sarkar I, Arora MK, Csaplovics E (2005) An approach for GIS-based statistical landslide susceptibility zonation with a case study in the Himalayas. Landslides 2:61–69

Saito H, Nakayama D, Matsuyama H (2009) Comparison of landslide susceptibility based on a decision-tree model and actual landslide occurrence: the Akaishi mountains, Japan. Geomorphology 109:108–121

Schuster RL, Fleming RW (1986) Economic losses and fatalities due to landslides. Bull Assoc Eng Geol 23:11–28

Sezer EA, Pradhan B, Gokceoglu C (2011) Manifestation of an adaptive neuro-fuzzy model on landslide susceptibility mapping: Klang valley, Malaysia. Expert Syst App 38(7):8208–8219

Sharifi MA, Herwijnen MV (2003) Spatial decision support systems. International Instiute for Geo-Information Science and Earth Observation (ITC). p 201

Sharifi MA, Retsios V (2004) Site selection for waste disposal through spatial multiple criteria decision analysis. J Telecommun Inf Technol 3:1–11

Shou KJ, Wang CF (2003) Analysis of the Chiufengershan landslide triggered by the 1999 Chi–Chi earthquake in Taiwan. Eng Geol 68:237–250

Tangestani MH (2009) A comparative study of dempster–shafer and fuzzy models for landslide susceptibility mapping using a GIS: an experience from zagros Mountains, SW Iran. J Asian Earth Sci 35:66–73

Van Den Eeckhaut M, Vanwalleghem T, Poesen J, Govers G, Verstraeten G, Vandekerckhove L (2006) Prediction of landslide susceptibility using rare events logistic regression: a case-study in the Flemish Ardennes (Belgium). Geomorphology 76:392–410

Van Westen CJ, Bonilla JBA (1990) Mountain hazard analysis using PC-based GIS. 6th IAEG Congress, vol 1. Balkema, Rotterdam, pp 265–271

Varnes DJ (1978) Slope movement types and processes. In: Schuster RL, Krizek RJ (eds) Landslides analysis and control. Special Report, Transportation Research Board. vol 176 National Academy of Sciences, New York, pp 12–33

Wan S (2009) A spatial decision support system for extracting the core factors and thresholds for landslide susceptibility map. Eng Geol 108:237–251

Wang R (2008) An expert knowledge-based approach to landslide susceptibility mapping using GIS and fuzzy logic, A dissertation submitted in partial fulfillment of the requirement for the degree of Docto of Philosophy, University of Wisconsin-Madison, p 175

Wilson JP, Gallant JC (2000) Terrain analysis principles and applications. Wiley, New York

Wood EF, Sivapalan M, Beven KJ (1990) Similarity and scale catchment storm response. Rev Geophisics 28:1–18

Yalcin A (2005) An investigation on Ardesen (Rize) region on the basis of landslide susceptibility, KTU, PhD Thesis (in Turkish)

Yalcin A (2008) GIS-based landslide susceptibility mapping using analytical hierarchy process and bivariate statistics in Anderson (Turkey): comparision of results and confirmations. Catena 1:1–12

Yeon YK, Han JG, Ryu KH (2010) Landslide susceptibility mapping in Injae, Korea, using a decision tree. Eng Geol 116:274–283

Yesilnacar E, Topal T (2005) Landslide susceptibility mapping: a comparison of logistic regression and neural networks methods in a medium scale study, Hendek region (Turkey). Eng Geol 79(3–4):251–266

Yilmaz I (2009) Landslide susceptibility mapping using frequency ratio, logistic regression, artificial neural networks and their comparison: a case study from kat landslides (Tokat-Turkey). Comp Geosci 35(6):1125–1138

Zhou G, Esaki T, Mitani Y, Xie M, Mori J (2003) Spatial probabilistic modeling of slope failure using an integrated GIS Monte Carlo simulation approach. Eng Geol 68:373–386

Zweig MH, Campbell G (1993) Receiver-operating characteristics (ROC) plots. Clin Chem 39: 561–577

http://www.springer.com/978-3-642-25494-9

Terrigenous Mass Movements
Detection, Modelling, Early Warning and Mitigation Using Geoinformation Technology
(Eds.)B. Pradhan; M. Buchroithner
2012, VIII, 398 p. 184 illus., 13 in color., Hardcover
ISBN: 978-3-642-25494-9